Effects of heavy-ion irradiation on FeSe

Yue Sun,[1,*] Akiyoshi Park,[1] Sunseng Pyon,[1] Tsuyoshi Tamegai,[1] Tadashi Kambara,[2] and Ataru Ichinose[3]

[1]*Department of Applied Physics, The University of Tokyo, 7-3-1 Hongo, Bunkyo-ku, Tokyo 113-8656, Japan*
[2]*Nishina Center, RIKEN, 2-1 Hirosawa, Wako, Saitama 351-0198, Japan*
[3]*Central Research Institute of Electric Power Industry, Electric Power Engineering Research Laboratory, 2-6-1,*
Nagasaka, Yokosuka-shi, Kanagawa 240-0196, Japan

We report the effects of heavy-ion irradiation on FeSe single crystals by irradiating uranium up to a dose-equivalent matching field of $B_\phi = 16$ T. Almost continuous columnar defects along the c axis with a diameter of ~ 10 nm are confirmed by high-resolution transmission electron microscopy. T_c is found to be suppressed by introducing columnar defects at a rate of $dT_c/dB_\phi \sim -0.29$ K/T, which is much larger than those observed in iron pnictides. This unexpected large suppression of T_c in FeSe is discussed in relation to the large diameter of the columnar defects as well as its unique band structure with a remarkably small Fermi energy. The critical current density is first dramatically enhanced with irradiation reaching a value over $\sim 2 \times 10^5$ A/cm^2 (~ 5 times larger than that of the pristine sample) at 2 K (self-field) with $B_\phi = 2$ T, then gradually suppressed with increasing B_ϕ. The δl pinning associated with charge-carrier mean-free-path fluctuations and the δT_c pinning associated with spatial fluctuations of the transition temperature are found to coexist in the pristine FeSe, while the irradiation increases the contribution from δl pinning and makes it dominant over $B_\phi = 4$ T.

I. INTRODUCTION

FeSe composed of only stacking Fe-Se layers [1] has the simplest crystal structure in iron-based superconductors (IBSs) and is usually regarded as the parent compound. It also manifests very intriguing properties such as the nematic state without long-range magnetic order [2], crossover from BCS to Bose-Einstein condensation (BEC) [3], a Dirac-cone-like state [4–6], and a quasi-two-dimensional Fermi surface at temperatures below the structure transition [7–9]. Recently, an unexpected high T_c with a sign of superconductivity over 100 K observed in monolayer FeSe [10] made this system a promising candidate for achieving high-temperature superconductivity and probing the mechanism of superconductivity.

To understand these intriguing properties and the unexpected high T_c in the FeSe system, it is crucial to know the gap structure, which is unfortunately still under debate. A nodal gap was reported based on the observation of the V-shaped scanning tunneling microscopy (STM) spectrum, a nearly linear temperature-dependent penetration depth at low temperatures, and a large residual thermal conductivity [3]. However, a nodeless gap structure is also claimed by the low-temperature specific heat [11,12], lower critical field, and thermal-conductivity measurements reported by other groups [13,14]. Such controversy may come from the difference in sample quality. Nodes in the superconducting gap of FeSe could be symmetry-unprotected accidental nodes [15]. Also, there have been few efforts for bulk FeSe to distinguish the interband sign-reversed $s_\pm$ state [16] and the sign-preserving s_{++} state [17].

Introduction of nonmagnetic scattering centers has been proved to be an effective method to identify the gap structures of novel superconductors [18–20]. By introducing point defects by light-particle irradiations, such as electrons and protons, a clear suppression of T_c was observed in both cuprates and iron pnictides and was attributed to the sign change of the order parameter in the d wave [18,21] and $s_\pm$ [22] (or competition between $s_\pm$ and s_{++} via inter- and intraband scatterings [23,24]), respectively. In the case of correlated disorders created by heavy-ion irradiation, such as columnar defects, an obvious suppression of T_c together with the increase in the normal-state resistivity has been reported in cuprates [25]. However, T_c shows only a small or nondetectable change in iron pnictides [26–33]. The temperature dependence of the penetration depth in Co- or K-substituted BaFe$_2$As$_2$ was found to change after heavy-ion irradiation, consistent with the $s_\pm$ scenario [29,30]. On the other hand, the columnar defects created by heavy-ion irradiation are also strong pinning centers due to the geometrical similarity to vortices, which have already been proved to be effective for the enhancement of critical current density J_c [26,27,31–33]. Their controllability is also advantageous in the study of vortex physics. Thus, studies of the effects of heavy-ion irradiation on FeSe are instructive for understanding its pairing mechanism and vortex physics, which is important for the application of this material.

Unfortunately, the effects of heavy-ion irradiation on pure FeSe is still left unexplored. In this paper, we report a systematic study of heavy-ion irradiation in high-quality FeSe single crystals by uranium irradiation. T_c is found to change sensitively with the density of columnar defects with an unexpectedly large suppression rate $dT_c/dB_\phi \sim -0.29$ K/T. The critical current density is first dramatically enhanced with irradiation up to a dose-equivalent matching field $B_\phi = 2$ T and then gradually suppressed with further increasing the dose. The origins of the large T_c suppression rate as well as the vortex pinning mechanism are discussed in detail.

II. EXPERIMENT

High-quality FeSe single crystals were grown using the vapor transport method [34]. Fe and Se powders were thoroughly mixed by grinding in a glove box for more than 30 min and were sealed in an evacuated quartz tube together

————
*sunyue@issp.u-tokyo.ac.jp

with a mixture of $AlCl_3$ and KCl powders. The quartz tube with chemicals was loaded into a horizontal tube furnace with one end heated up to $\sim$400 °C, while the other end was kept at $\sim$250 °C. After more than 35 days, single crystals with dimensions greater than 1×1 mm^2 can be obtained in the cold end. The obtained crystals are of high quality with a sharp superconducting transition width $\Delta T_c < 0.5$ K from susceptibility measurements and a large residual resistivity ratio of $\sim$33, as reported in our previous publications [6,35].

Single crystals used for the irradiation were selected from the same batch and were confirmed to show similar properties in the pristine state with negligible piece-dependent T_c and J_c. Before the irradiation, single crystals were cleaved to thin plates with a thickness of $\sim$20 μm along the c axis, which is much smaller than the projected range of 2.6 GeV uranium for FeSe of $\sim$60 μm, calculated by SRIM-2008 (the Stopping and Range of Ions in Matter-2008) [36]. The 2.6 GeV uranium was irradiated parallel to the c axis of the crystal at room temperature. The uranium irradiation up to a dose-equivalent magnetic field called the matching field B_ϕ of 16 T was performed at the RI Beam Factory operated by RIKEN Nishina Center and the Center for Nuclear Study of The University of Tokyo. The structure of the crystal was characterized by means of x-ray diffraction (XRD) with Cu Kα radiation. Cross-sectional observations of the irradiated FeSe were performed with high-resolution scanning transmission electron microscopy (STEM; JEOL, JEM-3000F). Magnetization measurements were performed using a commercial superconducting quantum interference device magnetometer (MPMS-XL5, Quantum Design).

III. RESULTS AND DISCUSSION

Figure 1(a) shows the single-crystal XRD patterns for FeSe before and after irradiation by uranium with $B_\phi = 2$ and 8 T. Only the (00l) peaks are observed, suggesting that the crystallographic c axis is perfectly perpendicular to the plane of the single crystals. After the irradiation, the positions of the (00l) peaks are almost unchanged from those in the pristine sample, which can be seen more clearly in the enlarged part of (003) peaks shown in the inset of Fig. 1(a). The almost identical XRD patterns of the crystals before and after the irradiation indicate that the columnar defects along the c axis created by uranium irradiation do not affect the lattice constant c.

Figure 1(b) shows a STEM image of the cross section along the c axis in FeSe irradiated by uranium with $B_\phi = 2$ T, where we can clearly identify that the morphology of defects along the projectile has a columnar shape (black lines, as pointed out in the figure) and is almost continuous along the c axis. A typical high-resolution STEM observation of the defect shown in the inset of Fig. 1(b) reveals that the diameter of the columnar defects in the irradiated FeSe is $\sim$10 nm. This size is very close to that of the amorphous columnar defects in high-temperature cuprate superconductors but much larger than that of $\sim$2–5 nm in Au-irradiated Ba(Fe$_{0.93}$Co$_{0.07}$)$_2$As$_2$ [26]. Actually, the shape and size of the columnar defects created by the irradiation are dependent not only on the mass and energy of the ions but also on the properties of the crystal itself, such as the thermal conductivity and carrier density [37].
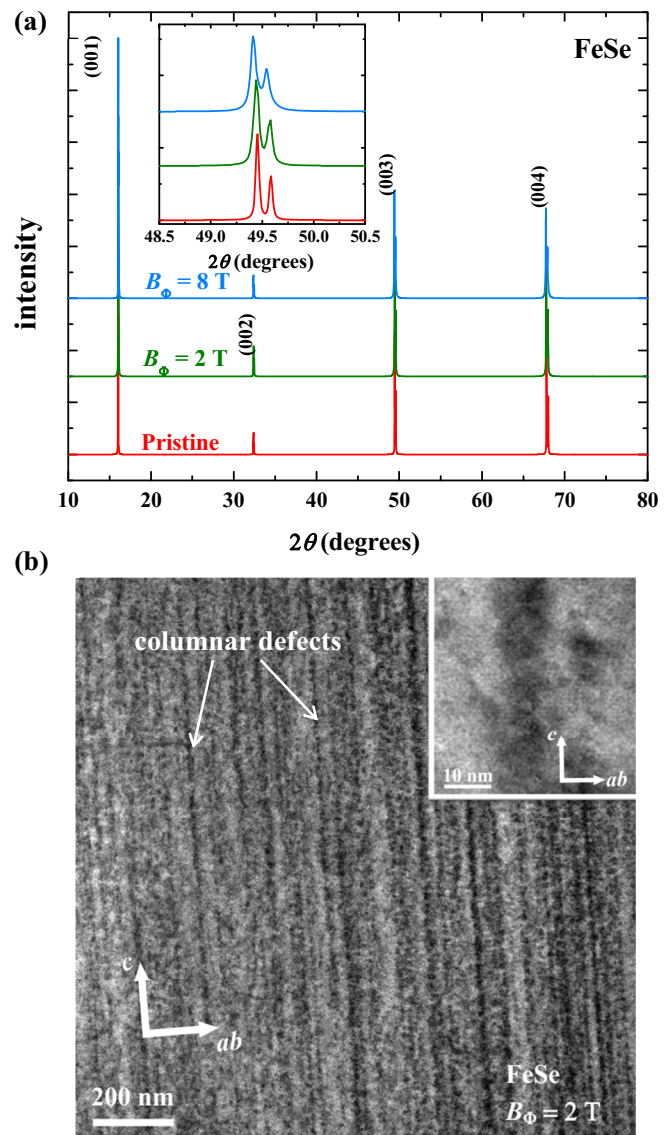

FIG. 1. (a) X-ray diffraction patterns for the FeSe single crystals before and after the irradiation by uranium with $B_\phi = 2$ and 8 T. The inset is an enlarged part of the (003) peaks. (b) Cross-sectional STEM micrograph of FeSe irradiated by uranium with $B_\phi = 2$ T. The inset shows an enlarged view of one of the columnar defects.

According to the study by Szenes [38] based on magnetic insulators, the radius of the columnar defects R_0 created by the heavy-ion irradiation can be expressed by

$$R_0^2 = a^2(0) \ln(S_e/S_{et}), \quad 2.7 \geqslant S_e/S_{et} \geqslant 1, \qquad (1)$$

$$R_0^2 = [a^2(0)/2.7](S_e/S_{et}), \quad S_e/S_{et} \geqslant 2.7, \qquad (2)$$

where S_e is the electronic stopping power, S_{et} is the threshold value, and $a(0)$ is related to the thermal diffusivity. Equation (1) is the situation for R_0 smaller than $\sim$1 nm, while Eq. (2) is the case for larger R_0, as shown in Fig. 1 of Ref. [38]. If we simply apply the above expression to the IBSs, the radius R_0 is proportional to $a(0)(S_e/S_{et})^{1/2}$ since the value of R_0 in IBSs is found to be in the range of $\sim$2–10 nm. The values of S_e
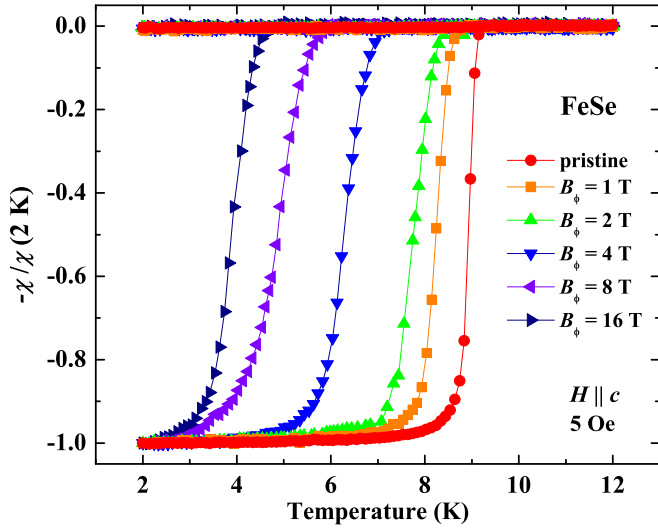
FIG. 2. Temperature dependence of the reduced magnetic susceptibilities $-\chi/\chi(2\,\mathrm{K})$ at 5 Oe for the pristine and uranium-irradiated FeSe with $B_\phi = 1, 2, 4, 8$, and 16 T.

can be calculated using the SRIM program and are comparable for 2.6 GeV uranium-irradiated BaFe$_2$As$_2$ ($\sim$4.8 keV/Å) and FeSe ($\sim$4.2 keV/Å). The threshold value S_{et} is expressed as $S_{et} = \rho\pi c a^2(0)T_0/g$, where ρ is the density, c is the specific heat, g is a constant, and $T_0 = T_m - T_{tg}$ is the difference between the melting temperature T_m and the target temperature T_{tg} [38]. Substituting the expression of S_{et} into Eq. (2), the prefactor $a(0)$ can be canceled, and R_0 is found to be proportional to $[S_e/\rho c(T_m - T_{tg})]^{1/2}$. The values of ρ are $\sim$5.9 and $\sim$4.7 g/cm^3 for BaFe$_2$As$_2$ and FeSe, respectively. The values of c/T at 200 K are $\sim$1.51 mJ/g K^2 (600 mJ/mol K^2) for BaFe$_2$As$_2$ [39] and $\sim$1.78 mJ/g K^2 (240 mJ/mol K^2) for FeSe [40]. The T_m of FeSe is $\sim$1238 K [41], while it is reported to be above 1443 K for BaFe$_2$As$_2$ [42]. T_{tg} is $\sim$300 K for both cases since the irradiation was performed at room temperature. Putting all the values listed above into Eq. (2), we can roughly estimate that R_0(FeSe)$/R_0$(BaFe$_2$As$_2$) > 1.14, the trend of which is consistent with the STEM observation.

Figure 2 shows the temperature dependence of the normalized magnetic susceptibilities $-\chi/\chi(2\,\mathrm{K})$ at 5 Oe for the pristine and uranium-irradiated FeSe with $B_\phi = 1, 2, 4, 8$, and 16 T. The pristine FeSe displays a superconducting transition temperature $T_c \sim 9.2$ K, which is evidently suppressed gradually with increasing B_ϕ. When $B_\phi = 16$ T, the value of T_c is reduced to below 5 K. On the other hand, the sharp superconducting transition width observed in the pristine crystal changes little after the irradiation, which confirms that the effect of columnar defects on superconductivity is homogeneous.

To study the effects of columnar defects on the critical current density, we first measured magnetic hysteresis loops (MHLs) at several temperatures for the pristine and uranium-irradiated crystals. Typical results for the MHLs for the pristine and irradiated crystals with $B_\phi = 1, 2, 4$, and 8 T are depicted in Figs. 3(a)–3(e), respectively. All the MHLs are almost symmetric, indicating that the bulk pinning is dominant in all crystals. However, the shape of the MHLs is obviously changed after the irradiation, especially the central peak around zero field. For the pristine crystal, a sharp central peak is observed, but it becomes broader after the irradiation, and a small diplike behavior can be observed near zero field in the crystals with $B_\phi = 1$ and 2 T. After a further increase in the density of columnar defects, the broader central peak becomes sharper again as in the crystals with $B_\phi = 4$ and 8 T.

The shape change in MHLs after irradiation can be seen more clearly in the scaled plot. As has been demonstrated in several superconductors, the MHLs at different temperatures can be well scaled onto one curve by choosing appropriate reducing parameters M^* and H^* if one single pinning mechanism is dominant [43–46]. The scaled MHLs at several temperatures for the pristine and uranium-irradiated FeSe with typical doses of $B_\phi = 2$ and 8 T are shown in Figs. 4(a)–4(c), respectively. The parameter M^* is selected as the maximum value of the magnetization, and H^* is the irreversibility field obtained by extrapolating J_c to zero in $J_c^{1/2}$ vs H curves [35]. For the pristine crystal, the MHLs measured at different temperatures can be well scaled, which is consistent with our previous report that FeSe is dominated by
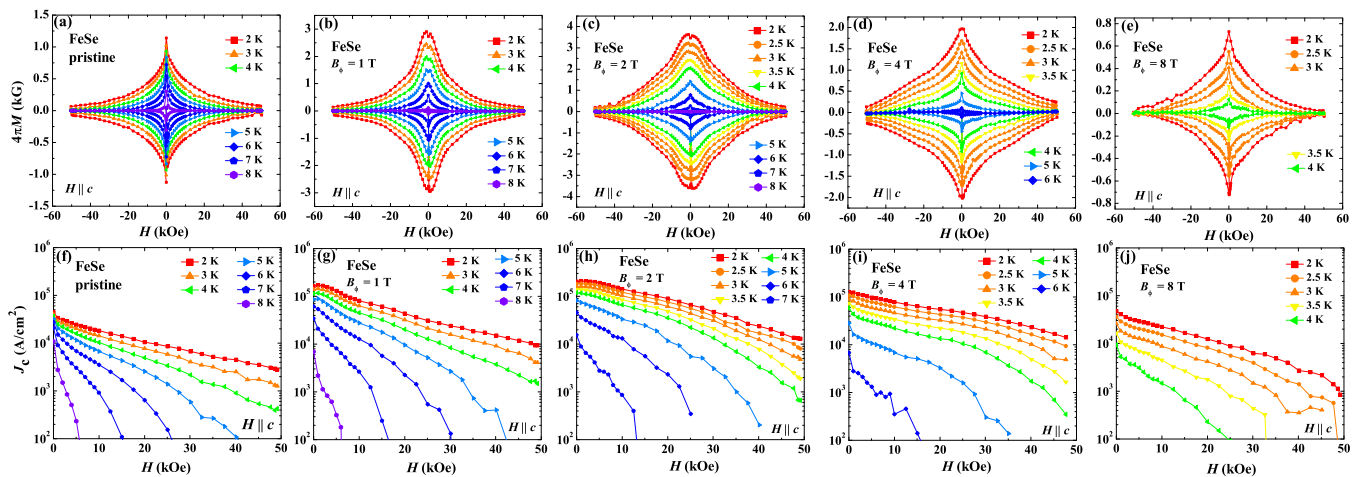

FIG. 3. Magnetic hysteresis loops at different temperatures for (a) pristine FeSe and (b)–(e) uranium-irradiated FeSe with $B_\phi = 1, 2, 4$, and 8 T, respectively. (f)–(j) The corresponding magnetic-field-dependent critical current densities.
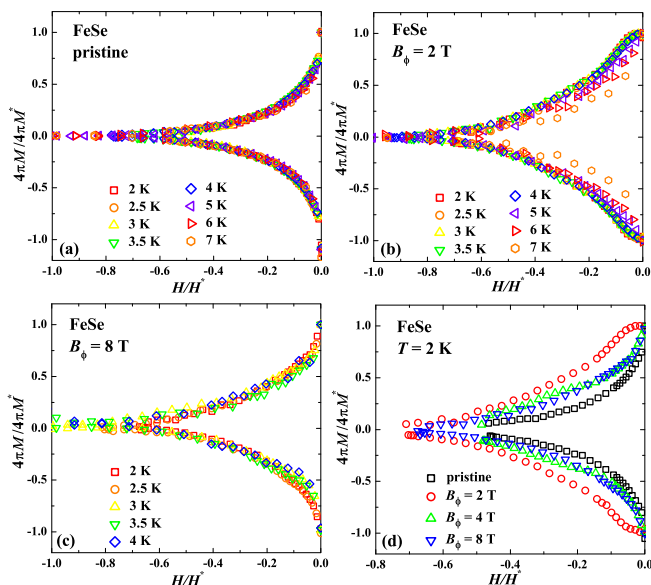
FIG. 4. Scaled MHLs for (a) pristine FeSe and (b) and (c) uranium-irradiated FeSe with $B_\phi = 2$ and 8 T, respectively, at different temperatures. (d) Scaled MHLs at 2 K for the pristine and irradiated crystals with $B_\phi = 2$, 4, and 8 T.

FIG. 5. Normalized T_c (T_c/T_{c0}, where T_{c0} is the value of T_c for the pristine one) and the self-field J_c at 2 K as a function of the matching field B_ϕ (bottom axis) and damaged area (top axis) for the uranium*irradiated FeSe. The inset is the evolution of T_c/T_{c0} and self-field J_c at 2 K as a function of the matching field B_ϕ for 2.6 GeV uranium-irradiated Ba$_{0.6}$K$_{0.4}$Fe$_2$As$_2$ (data obtained from Ref. [49]).

sparse, strong, pointlike pinning from nanometer-size defects or imperfections [35]. After introducing columnar defects by uranium irradiation, which are strong pinning centers in nature and pin the vortices strongly, as discussed above, two kinds of strong pinnings coexist in the crystal. Thus, the scaling of MHLs fails in the irradiated crystals, and one typical result for the crystal with $B_\phi = 2$ T was shown in Fig. 4(b). When the value of B_ϕ is increased larger than the maximum applied field of $\sim$5 T in the current experiment, all the vortices can be pinned by the columnar defects. In this case, only one kind of pinning center is dominant, i.e., the columnar defects, which makes the scaling of MHLs valid again, as seen in Fig. 4(c) for the crystal with $B_\phi = 8$ T. The shape change in MHLs caused by the irradiation can be seen more directly in Fig. 4(d), which shows the scaled MHLs at 2 K for the pristine and irradiated crystals with $B_\phi = 2$, 4, and 8 T. Such structural evolution in MHLs indicates the change in the pinning mechanism accompanied by the irradiation, which will be discussed in detail later.

Before discussing the origin of the shape change observed in MHLs, we first calculate the critical current density J_c from the MHLs by using the extended Bean model [47],

$$J_c = 20 \frac{\Delta M}{a(1 - a/3b)}, \qquad (3)$$

where ΔM is $M_{down} - M_{up}$, M_{up} (emu/cm^3) and M_{down} (emu/cm^3) are the magnetizations when sweeping fields up and down, respectively, and a (cm) and b (cm) are sample widths ($a < b$). The magnetic field dependence of J_c for the pristine and irradiated crystals with $B_\phi = 1$, 2, 4, and 8 T is shown in Figs. 3(f)–3(j), respectively. Obviously, the value of J_c is enhanced after introducing the columnar defects and reaches the maximum value for $B_\phi = 2$ T. For B_ϕ larger than 2 T, the value of J_c decreases with further increase in dose.
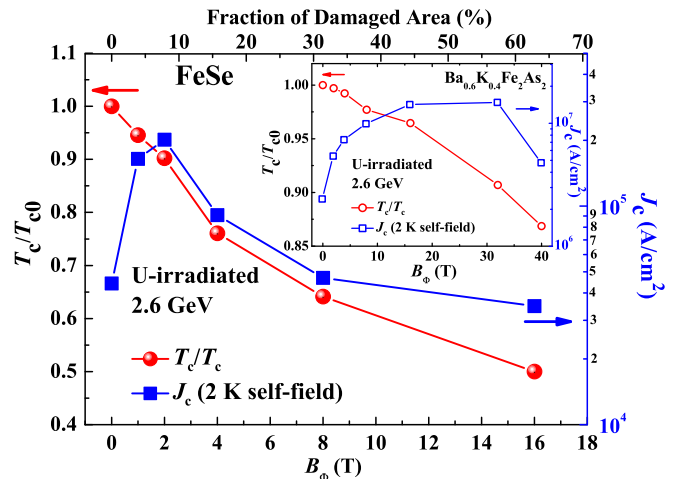
Now, we turn back to the discussion of the shape change in the MHLs after the irradiation. The broad central peak accompanied by a diplike structure in MHLs observed in samples with strong correlated pinning along the c axis is explained by the self-field (H_{sf}) effect [27,48]. When the magnetic field is smaller than H_{sf}, flux lines in a thin sample are strongly curved, which makes the pinning by columnar defects ineffective in large areas of the crystal and hence reduces the irreversible magnetization. When the field is increased to $H \sim H_{sf}$, the flux lines are straightened up in the sample. Thus, the pinning by columnar defects becomes effective, and irreversible magnetization reaches the maximum value. This scenario can explain the dip structure in MHLs of crystals with $B_\phi = 1$ and 2 T, where the self-field reaches the maximum value ($H_{sf} \propto J_c t$, where t is the thickness and is $\sim$20 μm for all the crystals). Actually, the location of the peak in MHLs at $\sim$1 kOe in the crystal with $B_\phi = 2$ T at 2 K roughly agrees with the self-field at 2 K for this crystal of $\sim$0.5 kG. When B_ϕ is increased larger than 2 T, the value of J_c is decreased, which makes H_{sf} too small to cause the diplike structure, while the central peak is still broader than the pristine one.

The effects of columnar defects are summarized by the normalized T_c and the self-field J_c at 2 K as a function of B_ϕ, as shown in Fig. 5. T_c is determined by the onset of diamagnetism for the zero-field-cooled susceptibility shown in Fig. 2. Evidently, the value of T_c is considerably suppressed with increasing B_ϕ, and the suppression of T_c is roughly in a linear function, with a slope of $dT_c/dB_\phi \simeq 3.2\% T_c$ T^{-1} (-0.29 K/T), which is much larger than other IBSs [27]. To directly show the differences between the heavy-ion irradiation effects on FeSe and iron pnictides, we also plot the evolution of T_c and J_c with increasing B_ϕ for the 2.6 GeV uranium-irradiated Ba$_{0.6}$K$_{0.4}$Fe$_2$As$_2$ in the inset of Fig. 5. The data are obtained from Ref. [49]. Obviously, the value of T_c is suppressed less than 5% in Ba$_{0.6}$K$_{0.4}$Fe$_2$As$_2$ for $B_\phi = 16$ T,

which is about one order smaller than that of ~50% in FeSe, suggesting a unique pairing mechanism for FeSe.

Before discussing the unexpectedly large T_c suppression rate by uranium irradiation in FeSe, it is worth noticing that the heavy-ion irradiation not only creates columnar defects but may also produce secondary energetic electrons as they lose energy. The secondary electron irradiation can introduce pointlike defects, which may act as a pairing breaker and suppress T_c unless the gap structure is an isotropic s wave. Such an effect is indeed observed in YBa$_2$Cu$_3$O$_{7-\delta}$ thin films [50] and in similar compounds such as FeTe$_{1-x}$Se$_x$ [51]. However, the electron irradiation has already been reported not to suppress T_c of FeSe, and instead, an unexpected small enhancement of T_c was observed [52]. Hence, the large T_c suppression observed here cannot be explained by the effect of the secondary electron irradiation. The large T_c suppression rate may originate from the much larger damaged areas after the heavy-ion irradiation. As shown in the inset of Fig. 1(b), the diameter of the columnar defects in the irradiated FeSe is ~10 nm, which is much larger than the ~2–5 nm observed in the irradiated IBS "122" system [26,27]. In such a case, the damaged areas in FeSe are ~4–25 times larger than those in the IBS 122 system. The fraction of the damaged area without considering the overlap between the defects is also plotted in Fig. 4 on the top axis. Obviously, the fraction of the damaged area reaches over 60% for $B_\phi = 16$ T. In addition, the coherence length of FeSe is ~4.5 nm [1], larger than the ~2–3 nm for the 122 system [53], which indicates that the defect areas in FeSe have more influence in the superconducting regions.

Recent STM observations showed that twin boundaries in FeSe may act as pairing breakers, which lift the nodes in their neighborhood and have long-range effects more than one order larger than the coherence length [54]. The nodes were found to be totally suppressed in the region between two neighboring twin boundaries of ~34 nm, which is close to the average distance between columnar defects at $B_\phi = 2$ T. Columnar defects may have effects similar to those of twin boundaries since they are both correlated defects and the widths of the damaged areas are similar. The proximity effect between the normal electrons in the damaged region and the Cooper pairs in the superconducting region may be responsible for the suppression of T_c. The much larger suppression of T_c in FeSe compared to other irradiated IBSs may also be related to its unique band structures, where the Fermi energy E_F is remarkably small and is comparable to the superconducting gap, suggesting that FeSe is in the crossover regime from BCS to BEC [3]. Such an extremely small E_F could be more sensitive to the defects than the large E_F in other IBSs. Local STM observations of the irradiated FeSe are required to clarify this issue and to find out if the behavior of T_c being sensitive to correlated defects is the common feature of the superconductors residing in the crossover regime from BCS to BEC.

On the other hand, the value of J_c is enhanced dramatically with the irradiation for $B_\phi \leqslant 2$ T. As also shown in Fig. 5 (right axis), the self-field J_c at 2 K is increased about 5 times from ~4×10^4 A/cm^2 for the pristine crystal to ~2×10^5 A/cm^2 for the crystals with $B_\phi = 2$ T. Such a large value of enhanced J_c is already close to that reported in high-quality FeTe$_{1-x}$Se$_x$ single crystals [55,56]. For $B_\phi > 2$ T, the value
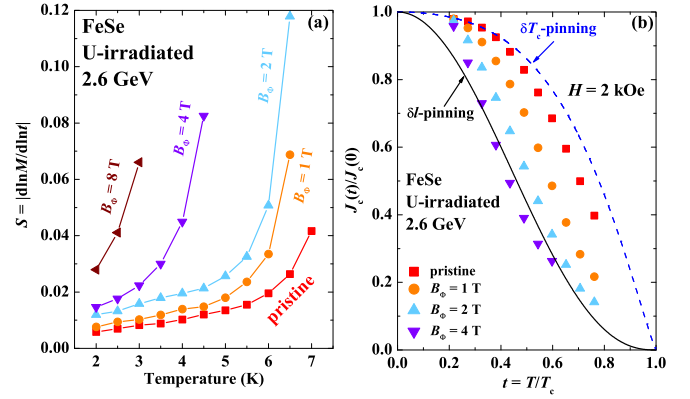

FIG. 6. (a) Temperature dependence of magnetic relaxation rate S measured at 2 kOe for the pristine and uranium-irradiated FeSe with $B_\phi = 1$, 2, 4, and 8 T. (b) Normalized critical current density $J_c(t)/J_c(0)$ at 2 kOe as a function of the reduced temperature $t = T/T_c$ for the pristine and uranium-irradiated FeSe with $B_\phi = 1$, 2, and 4 T. The solid and dashed lines are the theoretical curves for δl and δT_c pinnings.

of J_c is gradually suppressed with the increase in columnar defects. A similar evolution of J_c with increasing columnar defects is also observed in (Ba$_{0.6}$K$_{0.4}$)Fe$_2$As$_2$ [49]. As shown in the inset of Fig. 5, the value of J_c for (Ba$_{0.6}$K$_{0.4}$)Fe$_2$As$_2$ is also enhanced maximally about 5–6 times after uranium irradiation, although its absolute value is larger. Then, the value of J_c decreases with a further increase in dose. However, the maximum J_c in the irradiated (Ba$_{0.6}$K$_{0.4}$)Fe$_2$As$_2$ is observed with B_ϕ in the range of 20–30 T, which is one order larger than that of FeSe. The nature of the quick enhancement of J_c by a small dose of heavy-ion irradiation in FeSe is also advantageous for real applications. Although the value of J_c for the pure FeSe single crystal is relatively small, Te-doped FeSe tapes with J_c greater than 10^6 A/cm^2 under self-field and greater than 10^5 A/cm^2 under 30 T at 4.2 K have already been fabricated, which is promising for applications [57]. Recently, 1.5 times enhancement of J_c was achieved in a FeTe$_{0.5}$Se$_{0.5}$ thin film by irradiating it with protons [58]. Our current results indicate that heavy-ion irradiation with a small dose may be effective in the further enhancement of J_c for tapes and thin films of the FeSe system.

Major pinning mechanisms in type-II superconductors can be classified into two types: the δl pinning associated with charge-carrier mean-free-path fluctuations and the δT_c pinning associated with spatial fluctuations of the transition temperature. The typical temperature dependences of J_c for the δl pinning and δT_c pinning are given by $J_c(t)/J_c(0) = (1 - t^2)^{5/2}(1 + t^2)^{-1/2}$ and $J_c(t)/J_c(0) = (1 - t^2)^{7/6}(1 + t^2)^{5/6}$, respectively [59]. To compare the J_c obtained from the MHLs with the theoretical estimation, we need to consider the magnetic relaxation since there is a finite time delay between the measurement and the preparation of the critical state and the relaxation rate has been reported to be large in FeSe [35]. The decay of magnetization with time was traced for more than 1 h from the moment when the critical state was prepared. The normalized magnetic relaxation rate S can be obtained from $S = |d\ln M/d\ln t|$ and is shown in Fig. 6(a) for the pristine and uranium-irradiated crystals with $B_\phi = 1, 2, 4$, and 8 T measured

under 2 kOe. The temperature dependence of S shows an obvious crossover from a temperature-insensitive plateau with a small slope to a steep increase, which is attributed to the crossover from the elastic to plastic creep [35]. After the uranium irradiation, the crossover is gradually suppressed to lower temperatures, and the plateau region cannot be observed above 2 K in the crystal with $B_\phi = 8$ T, which is related to the suppression of T_c. With the values of S, we can calculate the (true) J_c without flux creep using the generalized inversion scheme with parameters for the three-dimensional single-vortex pinning [60,61].

The temperature dependence of J_c is normalized by the value of $J_c(0)$ obtained from the extended Maley's method [62] as already performed for the pristine FeSe shown in our previous publication [35]. The temperature dependence of the normalized J_c for the pristine and uranium-irradiated FeSe with $B_\phi = 1$, 2, and 4 T is shown in Fig. 6(b) together with the theoretical curves for δl and δT_c pinnings. For the pristine crystal, $J_c(t)$ resides between the predictions for the δl and δT_c pinnings, closer to the curve for the δT_c pinning, especially at low temperatures. The fact that temperature dependence of the normalized J_c resides between the δT_c and δl pinning curves indicates both pinning mechanisms may coexist in the pristine FeSe, similar to what was reported for FeTe$_{0.6}$Se$_{0.4}$ [63], Co-doped BaFe$_2$As$_2$ [64,65], and K-doped BaFe$_2$As$_2$ [66], and the δT_c pinning is more dominant in the pristine crystal. The main pinning centers in the pristine FeSe are found to be nanometer-size defects or imperfections, as reported in our previous publication [35] and also observed by the STM observations [3]. Such defects or imperfections

will enhance the spatial variation of the mean free path and hence contribute to the δl pinning. On the other hand, those defects or imperfections mainly originate from the Fe nonstoichiometries [67]. Since the value of T_c for FeSe is very sensitive to the stoichiometry of Fe to Se [67], those defects or imperfections will also cause spatial fluctuations of T_c, which contribute to the δT_c pinnings. After uranium irradiation, mean-free-path fluctuations should increase since more defects are introduced. As expected, the temperature dependence of J_c gradually approaches the theoretical curve for δl pinnings with the increase in B_ϕ. For $B_\phi = 4$ T, it almost falls onto the curve for the δl pinning except for the low-temperature part, which means that the pinning associated with charge-carrier mean-free-path fluctuations becomes dominant.

IV. CONCLUSIONS

In summary, we reported a systematic study of the effects of columnar defects on FeSe single crystals by uranium irradiations. T_c was found to be suppressed by columnar defects at the large rate of $dT_c/dB_\phi \sim -0.29$ K/T. The unexpected large suppression of T_c in FeSe was discussed in relation to the large diameter of the columnar defects as well as its unique band structure with a remarkably small Fermi energy. The critical current density is first dramatically enhanced with irradiation, reaching a value more than $\sim 2 \times 10^5$ A/cm^2 at 2 K (self-field) for $B_\phi = 2$ T, then is gradually suppressed with increasing B_ϕ. The coexistence of δl and δT_c pinnings in the pristine FeSe (δT_c pinnings are more dominant) is turned into dominant δl pinnings after the irradiation.

[1] F. C. Hsu, J. Y. Luo, K. W. Yeh, T. K. Chen, T. W. Huang, P. M. Wu, Y. C. Lee, Y.-L. Huang, Y.-Y. Chu, D. C. Yan, and M. K. Wu, Proc. Natl. Acad. Sci. USA **105**, 14262 (2008).

[2] T. M. McQueen, A. J. Williams, P. W. Stephens, J. Tao, Y. Zhu, V. Ksenofontov, F. Casper, C. Felser, and R. J. Cava, Phys. Rev. Lett. **103**, 057002 (2009).

[3] S. Kasahara, T. Watashige, T. Hanaguri, Y. Kohsaka, T. Yamashita, Y. Shimoyama, Y. Mizukami, R. Endo, H. Ikeda, K. Aoyama, T. Terashima, S. Uji, T. Wolf, H. von Löhneysen, T. Shibauchi, and Y. Matsuda, Proc. Natl. Acad. Sci. USA **111**, 16309 (2014).

[4] S. Onari, Y. Yamakawa, and H. Kontani, Phys. Rev. Lett. **116**, 227001 (2016).

[5] Y. Zhang, M. Yi, Z. K. Liu, W. Li, J. J. Lee, R. G. Moore, M. Hashimoto, N. Masamichi, H. Eisaki, S. K. Mo, Z. Hussain, T. P. Devereaux, Z. X. Shen, and D. H. Lu, Phys. Rev. B **94**, 115153 (2016).

[6] Y. Sun, S. Pyon, and T. Tamegai, Phys. Rev. B **93**, 104502 (2016).

[7] M. D. Watson, T. K. Kim, A. A. Haghighirad, N. R. Davies, A. McCollam, A. Narayanan, S. F. Blake, Y. L. Chen, S. Ghannadzadeh, A. J. Schofield, M. Hoesch, C. Meingast, T. Wolf, and A. I. Coldea, Phys. Rev. B **91**, 155106 (2015).

[8] T. Terashima, N. Kikugawa, A. Kiswandhi, E.-S. Choi, J. S. Brooks, S. Kasahara, T. Watashige, H. Ikeda, T. Shibauchi, Y. Matsuda, T. Wolf, A. E. Böhmer, F. Hardy, C. Meingast, H. v. Löhneysen, M.-T. Suzuki, R. Arita, and S. Uji, Phys. Rev. B **90**, 144517 (2014).

[9] Y. Sun, T. Yamada, S. Pyon, and T. Tamegai, Phys. Rev. B **94**, 134505 (2016).

[10] J. F. Ge, Z. L. Liu, C. Liu, C. L. Gao, D. Qian, Q. K. Xue, Y. Liu, and J. F. Jia, Nat. Mater. **14**, 285 (2015).

[11] J. Y. Lin, Y. S. Hsieh, D. A. Chareev, A. N. Vasiliev, Y. Parsons, and H. D. Yang, Phys. Rev. B **84**, 220507 (2011).

[12] J. Lin, C. Huang, S. Rößler, C. Koz, U. K. Rößler, U. Schwarz, and S. Wirth, Sci. Rep. **7**, 44024 (2017).

[13] J. K. Dong, T. Y. Guan, S. Y. Zhou, X. Qiu, L. Ding, C. Zhang, U. Patel, Z. L. Xiao, and S. Y. Li, Phys. Rev. B **80**, 024518 (2009).

[14] P. Bourgeois-Hope, S. Chi, D. A. Bonn, R. Liang, W. N. Hardy, T. Wolf, C. Meingast, N. Doiron-Leyraud, and L. Taillefer, Phys. Rev. Lett. **117**, 097003 (2016).

[15] A. Kreisel, S. Mukherjee, P. J. Hirschfeld, and B. M. Andersen, Phys. Rev. B **92**, 224515 (2015).

[16] I. I. Mazin, D. J. Singh, M. D. Johannes, and M. H. Du, Phys. Rev. Lett. **101**, 057003 (2008).

[17] H. Kontani and S. Onari, Phys. Rev. Lett. **104**, 157001 (2010).

[18] H. Alloul, J. Bobroff, M. Gabay, and P. J. Hirschfeld, Rev. Mod. Phys. **81**, 45 (2009).

[19] Y. Nakajima, T. Taen, Y. Tsuchiya, T. Tamegai, H. Kitamura, and T. Murakami, Phys. Rev. B **82**, 220504 (2010).

[20] T. Taen, F. Ohtake, H. Akiyama, H. Inoue, Y. Sun, S. Pyon, T. Tamegai, and H. Kitamura, Phys. Rev. B **88**, 224514 (2013).

[21] F. Rullier-Albenque, D. Colson, A. Forget, and H. Alloul, Phys. Rev. Lett. **109**, 187005 (2012).

[22] Y. Wang, A. Kreisel, P. J. Hirschfeld, and V. Mishra, Phys. Rev. B **87**, 094504 (2013).

[23] T. Saito, S. Onari, and H. Kontani, Phys. Rev. B **88**, 045115 (2013).

[24] H. Hosono and K. Kuroki, Physica C (Amsterdam, Neth.) **514**, 399 (2015).

[25] D. Bourgault, S. Bouffard, M. Toulemonde, D. Groult, J. Provost, F. Studer, N. Nguyen, and B. Raveau, Phys. Rev. B **39**, 6549 (1989).

[26] Y. Nakajima, Y. Tsuchiya, T. Taen, T. Tamegai, S. Okayasu, and M. Sasase, Phys. Rev. B **80**, 012510 (2009).

[27] T. Tamegai, T. Taen, H. Yagyuda, Y. Tsuchiya, S. Mohan, T. Taniguchi, Y. Nakajima, S. Okayasu, M. Sasase, H. Kitamura, T. Murakami, T. Kambara, and Y. Kanai, Supercond. Sci. Technol. **25**, 084008 (2012).

[28] H. Kim, R. T. Gordon, M. A. Tanatar, J. Hua, U. Welp, W. K. Kwok, N. Ni, S. L. Bud'ko, P. C. Canfield, A. B. Vorontsov, and R. Prozorov, Phys. Rev. B **82**, 060518(R) (2010).

[29] J. Murphy, M. A. Tanatar, H. Kim, W. Kwok, U. Welp, D. Graf, J. S. Brooks, S. L. Bud'ko, P. C. Canfield, and R. Prozorov, Phys. Rev. B **88**, 054514 (2013).

[30] N. W. Salovich, H. Kim, A. K. Ghosh, R. W. Giannetta, W. Kwok, U. Welp, B. Shen, S. Zhu, H. H. Wen, M. A. Tanatar, and R. Prozorov, Phys. Rev. B **87**, 180502 (2013).

[31] L. Fang, Y. Jia, C. Chaparro, G. Sheet, H. Claus, M. A. Kirk, A. E. Koshelev, U. Welp, G. W. Crabtree, W. K. Kwok, S. Zhu, H. F. Hu, J. M. Zuo, H. H. Wen, and B. Shen, Appl. Phys. Lett. **101**, 012601 (2012).

[32] L. Fang, Y. Jia, V. Mishra, C. Chaparro, V. K. Vlasko-Vlasov, A. E. Koshelev, U. Welp, G. W. Crabtree, S. Zhu, N. D. Zhigadlo, S. Katrych, J. Karpinski, and W. K. Kwok, Nat. Commun. **4**, 2655 (2013).

[33] K. J. Kihlstrom, L. Fang, Y. Jia, B. Shen, A. E. Koshelev, U. Welp, G. W. Crabtree, W.-K. Kwok, A. Kayani, S. F. Zhu, and H.-H. Wen, Appl. Phys. Lett. **103**, 202601 (2013).

[34] A. E. Böhmer, F. Hardy, F. Eilers, D. Ernst, P. Adelmann, P. Schweiss, T. Wolf, and C. Meingast, Phys. Rev. B **87**, 180505(R) (2013).

[35] Y. Sun, S. Pyon, T. Tamegai, R. Kobayashi, T. Watashige, S. Kasahara, Y. Matsuda, and T. Shibauchi, Phys. Rev. B **92**, 144509 (2015).

[36] J. Ziegler, J. Biersack, and U. Littmark, *The Stopping and Range of Ions in Solids* (Pergamon, New York, 1985).

[37] Y. Zhu, Z. X. Cai, R. C. Budhani, M. Suenaga, and D. O. Welch, Phys. Rev. B **48**, 6436 (1993).

[38] G. Szenes, Phys. Rev. B **51**, 8026 (1995).

[39] C. R. Rotundu, B. Freelon, T. R. Forrest, S. D. Wilson, P. N. Valdivia, G. Pinuellas, A. Kim, J.-W. Kim, Z. Islam, E. Bourret-Courchesne, N. E. Phillips, and R. J. Birgeneau, Phys. Rev. B **82**, 144525 (2010).

[40] M. Abdel-Hafiez, Y. J. Pu, J. Brisbois, R. Peng, D. L. Feng, D. A. Chareev, A. V. Silhanek, C. Krellner, A. N. Vasiliev, and X.-J. Chen, Phys. Rev. B **93**, 224508 (2016).

[41] H. Okamoto, J. Phase Equilib. **12**, 383 (1991).

[42] R. Morinaga, K. Matan, H. S. Suzuki, and T. J. Sato, Jpn. J. Appl. Phys. **48**, 013004 (2009).

[43] G. K. Perkins, L. F. Cohen, A. A. Zhukov, and A. D. Caplin, Phys. Rev. B **51**, 8513 (1995).

[44] M. Oussena, P. A. J. de Groot, A. Marshall, and J. S. Abell, Phys. Rev. B **49**, 1484 (1994).

[45] C. D. Dewhurst, D. A. Cardwell, A. M. Campbell, R. A. Doyle, G. Balakrishnan, and D. M. Paul, Phys. Rev. B **53**, 14594 (1996).

[46] C. D. Dewhurst, R. A. Doyle, G. Balakrishnan, G. Wirth, and D. M. Paul, Phys. Rev. B **62**, 14373 (2000).

[47] C. P. Bean, Rev. Mod. Phys. **36**, 31 (1964).

[48] G. P. Mikitik and E. H. Brandt, Phys. Rev. B **62**, 6800 (2000).

[49] F. Ohtake, T. Taen, S. Pyon, T. Tamegai, S. Okayasu, T. Kambara, and H. Kitamura, Physica C (Amsterdam, Neth.) **518**, 47 (2015).

[50] R. Biswal, J. John, D. Behera, P. Mallick, K. Sandeep, D. Kanjilal, T. Mohanty, P. Raychaudhuri, and N. C. Mishra, Supercond. Sci. Technol. **21**, 085016 (2008).

[51] F. Massee, P. O. Sprau, Y. L. Wang, J. C. S. Davis, G. Ghigo, G. D. Gu, and W. K. Kwok, Sci. Adv. **1**, e1500033 (2015).

[52] S. Teknowijoyo, K. Cho, M. A. Tanatar, J. Gonzales, A. E. Böhmer, O. Cavani, V. Mishra, P. J. Hirschfeld, S. L. Bud'ko, P. C. Canfield, and R. Prozorov, Phys. Rev. B **94**, 064521 (2016).

[53] A. Gurevich, Rep. Prog. Phys. **74**, 124501 (2011).

[54] T. Watashige, Y. Tsutsumi, T. Hanaguri, Y. Kohsaka, S. Kasahara, A. Furusaki, M. Sigrist, C. Meingast, T. Wolf, H. v. Löhneysen, T. Shibauchi, and Y. Matsuda, Phys. Rev. X **5**, 031022 (2015).

[55] Y. Sun, T. Taen, Y. Tsuchiya, Q. Ding, S. Pyon, Z. X. Shi, and T. Tamegai, Appl. Phys. Express **6**, 043101 (2013).

[56] Y. Sun, Y. Tsuchiya, T. Taen, T. Yamada, S. Pyon, A. Sugimoto, T. Ekino, Z. X. Shi, and T. Tamegai, Sci. Rep. **4**, 4585 (2014).

[57] W. Si, S. J. Han, X. Shi, S. N. Ehrlich, J. Jaroszynski, A. Goyal, and Q. Li, Nat. Commun. **4**, 1347 (2013).

[58] T. Ozaki, L. Wu, C. Zhang, J. Jaroszynski, W. Si, J. Zhou, Y. Zhu, and Q. Li, Nat. Commun. **7**, 13036 (2016).

[59] R. Griessen, Wen Hai-hu, A. J. J. van Dalen, B. Dam, J. Rector, H. G. Schnack, S. Libbrecht, E. Osquiguil, and Y. Bruynseraede, Phys. Rev. Lett. **72**, 1910 (1994).

[60] H. G. Schnack, R. Griessen, J. G. Lensink, and W. Hai-Hu, Phys. Rev. B **48**, 13178(R) (1993).

[61] Wen Hai-hu, H. G. Schnack, R. Griessen, B. Dam, and J. Rector, Physica C (Amsterdam, Neth.) **241**, 353 (1995).

[62] L. Miu and D. Miu, Supercond. Sci. Technol. **23**, 025033 (2010).

[63] Y. Sun, T. Taen, Y. Tsuchiya, S. Pyon, Z. X. Shi, and T. Tamegai, Europhys. Lett. **103**, 57013 (2013).

[64] B. Shen, P. Cheng, Z. Wang, L. Fang, C. Ren, L. Shan, and H.-H. Wen, Phys. Rev. B **81**, 014503 (2010).

[65] T. Taen, Y. Nakajima, T. Tamegai, and H. Kitamura, Phys. Rev. B **86**, 094527 (2012).

[66] S. R. Ghorbani, X. L. Wang, M. Shahbazi, S. X. Dou, and C. T. Lin, Appl. Phys. Lett. **100**, 212601 (2012).

[67] T. M. McQueen, Q. Huang, V. Ksenofontov, C. Felser, Q. Xu, H. Zandbergen, Y. S. Hor, J. Allred, A. J. Williams, D. Qu, J. Checkelsky, N. P. Ong, and R. J. Cava, Phys. Rev. B **79**, 014522 (2009).